HHS Public Access

Author manuscript

Nat Biotechnol. Author manuscript; available in PMC 2015 October 01.

Published in final edited form as:

Nat Biotechnol. 2015 April ; 33(4): 390–394. doi:10.1038/nbt.3155.

Inducible *in vivo* genome editing with CRISPR/Cas9

Lukas E Dow[#1,2,*], **Jonathan Fisher**[#1], **Kevin P O'Rourke**[1,3], **Ashlesha Muley**[2], **Edward R Kastenhuber**[1,4], **Geulah Livshits**[1], **Darjus F Tschaharganeh**[1], **Nicholas D Socci**[5], and **Scott W Lowe**[1,6,*]

[1] Cancer Biology and Genetics Program, Memorial Sloan Kettering Cancer Center, New York, NY

[2] Hematology / Medical Oncology Division, Department of Medicine, Weill-Cornell Medical College, New York, NY

[3] Weill-Cornell / Rockefeller / Sloan Kettering Tri-Institutional MD-PhD program, New York, NY

[4] Gerstner Sloan Kettering Graduate School of Biomedical Sciences, New York, NY

[5] Bioinformatics Core facility, Memorial Sloan Kettering Cancer Center, New York, NY

[6] Howard Hughes Medical Institute, Memorial Sloan Kettering Cancer Center, New York, NY

[#] These authors contributed equally to this work.

Abstract

CRISPR/Cas9-based genome editing enables the rapid genetic manipulation of any genomic locus without the need for gene targeting by homologous recombination. Here we describe a conditional transgenic approach that allows temporal control of CRISPR/Cas9 activity for inducible genome editing in adult mice. We show that doxycycline-regulated Cas9 induction enables widespread gene disruption in multiple tissues and that limiting the duration of Cas9 expression or using a $Cas9^{D10A}$ (Cas9n) variant, can regulate the frequency and size of target gene modifications, respectively. Further, we show that the inducible CRISPR (iCRISPR) system can be used effectively to create biallelic mutation in multiple target loci and thus, provides a flexible and fast platform to study loss of function phenotypes *in vivo.*

Keywords

APC; polyposis; Cas9; CRISPR; genome editing

The type II bacterial CRISPR (clustered regularly interspaced short palindromic repeats)/ Cas9 system can be engineered to induce RNA-directed, double strand DNA breaks or

[*] Correspondence to: Lukas Dow: lud2005@med.cornell.edu Scott Lowe: lowes@mskcc.org.

Competing interest statement: The authors declare no competing financial interests

Author Contributions

LED conceived of the project, performed and analyzed experiments and wrote the paper. JF performed and analyzed experiments and wrote the paper. KPO, AM, GL and DFT performed and analyzed experiments. ERK and NDS developed informatics pipelines and analyzed data. SWL supervised experiments, analyzed data and wrote the paper.

single strand 'nicks' using a mutated form of Cas9 ($Cas9^{D10A}$ or Cas9n)[1-3]. CRISPR/Cas9 technology has been used to create heritable changes in the mouse genome, dramatically decreasing the time required to develop genetically engineered mouse models (GEMMs)[4-6]. However, homozygous germline mutations often result in embryonic lethality or developmental defects and are not tissue specific, limiting the utility of such models for studying gene function in adult tissues. Additionally, while CRISPR/Cas9 directed mutagenesis in zygotes enables rapid generation of compound mutants, genetic mosaicism in the founders and allele segregation limits the ability to produce large cohorts of experimental mice without further intercrossing. Here, we describe a rapid tetracycline (doxycycline)-regulated approach that enables inducible *in vivo* genetic manipulation of multiple loci from a single transgene.

We and others have previously used a recombinase-mediated cassette exchange approach to deliver tetracycline inducible cDNAs and shRNAs to a defined genomic locus, thus reducing founder effects associated with random integration [7,8]. As proof of principle, we chose to target the well characterized Adenomatous Polyposis Coli (Apc) tumor suppressor, as germline loss of Apc is embryonic lethal[9], while disruption of Apc in the intestine of adult mice results in the development of hyperplastic polyps[10]. We first generated single guide RNAs (sgRNAs) targeting murine *Apc* that contained a unique 'seed' region in the 12bp immediately upstream of the NGG PAM sequence (see Methods). We also developed sgRNAs to target *Trp53* (Supplementary Figure 1A), a gene whose inactivation often co-occurs with APC colon cancer. Analysis of transfected mouse ES cells using Surveyor assays showed the expected modifications (Supplementary Figure 1A). We next cloned each U6-sgRNA cassette into a new *col1a1*-targeting construct, upstream of TRE^{3G}-regulated GFP-IRES-Cas9 (Figure 1A), which facilitates the generation of constructs carrying multiple U6-sgRNA cassettes in series. As a control for sgRNA expression and Cas9-mediated DNA cleavage, we generated an sgRNA targeting a non-genic region on mouse chromosome 8 (*CR8*).

We produced KH2 ES cell clones targeting *CR8*, *Apc* and *Trp53* and tested for the presence of insertions and deletions (indels) by Surveyor assay. Both GFP induction (linked to Cas9) (Figure 1B) and target modification occurred within 2 days of dox treatment (Figure 1C) and increased with time (Figure 1D). In addition, targeted ES cell clones carrying both *Apc* and *Trp53* sgRNAs in tandem showed equivalent indel frequency (Figure 1C), indicating that the presence of two sgRNAs in series does not influence the efficiency of Cas9-mediated cleavage. To directly assess the capability of our system to induce biallelic modification in multiple genes, we treated two independent c3GIC9-*Apc/Trp53* parental ES clones with dox for 10 days, removed dox and allowed single clones to expand in the absence of Cas9 expression. Of 154 individual ESCs clones analyzed by Sanger sequencing, greater than 94% displayed biallelic disruption at a given locus (Figure 1E). Both alleles showed a frameshift-to-inframe indel ratio of close to 2:1 (expected by chance) (Figure 1F), implying that selection for loss-of-function mutations did not account for the high frequency of indels observed. Most importantly, more than 90% of all clones assessed showed biallelic modification at both *Apc* and *Trp53* (Figure 1G, left) and nearly half of all clones contained frameshift disruptions at each of the 4 alleles (Figure 1G, right). These data suggest that the

iCRISPR system can be used to induce disruption of multiple targets from a single transgene.

In some cases we identified ES cell clones that showed evidence of indels in the absence of dox (see asterisk, Figure 1C). Of 39 clones analysed, 13 (33%) displayed some level of off-dox mutagenesis. However, the frequency of 'off-dox' mutations did not increase with continuous culture (Figure 1D, see also [11]), suggesting they arise due to leaky expression of Cas9 during transfection. Thus, we screen up to 6 clones for each targeting event, to identify non-mutated clones for mouse production.

CRISPR/Cas9 genome editing can also cause 'off-target' mutations[12]. We identified potential off-target loci (Supplementary Table 1, see Methods) and assessed their mutation in dox-treated c3GIC9-*Apc/Trp53* ES cells. Of all off-target predictions for sg-*Trp53* (12 sites) and sg-*Apc* (6 sites) sgRNAs, only one of the *Trp53* predictions (an intron of *Elk3*) showed evidence of indels (Supplementary Figure 1B). This region was modified in every dox-treated Trp53 sgRNA clone (Supplementary Figure 1C), implying it is a bone fide off-target site. Of the 18 predicted off-targets, only OFT7 (*Elk3* intron) displayed 100% complementarity in the 12bp seed region upstream of the PAM (Supplementary Table 1), in line with previous observations and suggesting the 3' region of sgRNAs dictate target specificity [1].

Off-target mutagenesis can be reduced in cultured cells by using the Cas9n 'nickase' variant in combination with closely spaced sgRNAs targeting alternate DNA strands, providing increased specificity for the intended locus [3]. We cloned sgRNAs to pair with existing sgRNAs for *Apc* and *Trp53* (Supplementary Figure 1A), and generated targeted ES clones carrying each paired combination with a TRE^{3G} regulated Cas9n transgene. As expected, induction of Cas9n promoted indels for both *Trp53* (Supplementary Figure 1C) and *Apc* (Supplementary Figure 1D) but eliminated mutational events at the (*Elk3*) sg-*Trp53* off-target site (Supplementary Figure 1C). Our survey was not genome-wide, and thus we cannot rule out the possibility that there are other regions affected by the sgRNAs/Cas9 complexes. However, these data show that use of the 'paired nickase' approach can produce conditional knockouts while reducing undesired genomic modifications.

We next produced transgenic mice carrying c3GIC9 targeting *CR8*, *Apc* and *Apc/Trp53* as well c3GIC9n targeting *Apc* (Apc^n). Breeding of founders confirmed that each of the targeted alleles was transmitted in Mendelian ratios suggesting no toxicity during embryonic development (Supplementary Table 2). Still, even small amounts of leaky Cas9 expression would be expected to induce germline mutation events. Sequencing revealed that only 16/166 loci (9.6%) of the offspring carried heterozygous mutations in *CR8*, *Apc* or *Trp53*. Within each strain, these heterozygous mutations were identical, suggesting they arise from rare events in ESCs that contribute to the germline of the founder, rather than independent, spontaneous events during breeding. Thus, leaky Cas9 expression during ESC clone generation can occasionally induce dox-independent mutagenesis, but it is readily manageable by selecting appropriate F1 progeny for strain propagation.

Conditional deletion of *Apc* in the mouse intestine induces hyperplastic proliferation and blocks differentiation, leading to rapid intestinal dysfunction and death [13]. To determine whether the CRISPR/Cas9 system could recapitulate conditional *Apc* knockout phenotypes *in vivo*, we treated 4-5 week old R26-rtTA / c3GCI9 bi-transgenic animals with dox and monitored them over time. Surveyor analysis of intestinal villi following 10 days of dox showed expected gene alterations (Supplementary Figure 2A) and immunostaining confirmed Apc and p53 protein loss (Figure 2A). Of note, we observed some p53 positive cells and rare instances of increased staining, perhaps reflecting deletion of a region that regulates protein stability (Figure 2A, arrow). Those animals carrying *Apc*-targeted sgRNAs showed a 40-60 fold induction of the Wnt target genes Axin2 and Lgr5 and dramatic (130-fold) increase in the proto-oncogene cMyc (Supplementary Figure 2B). Mirroring the molecular response, histology revealed dramatic hyperproliferation, crypt expansion (Ki67 - green), a marked reduction in differentiation (Keratin 20 - red) and ectopic production of Lysozyme-positive Paneth cells (Figure 2B, Supplementary Figure 2C), as expected following acute deletion of Apc [13]. Surprisingly, the Cas9n/paired sgRNA approach was as efficient at producing *Apc* mutations as Cas9 (Supplementary Figure 2A), promoted a similar or greater increase in Wnt target gene expression (Supplementary Figure 2B), and produced an identical intestinal phenotype (Figure 2B).

To more closely evaluate iCRISPR function over time, we exploited the fact that Apc inactivation induces a measurable morphological (spheroid) change in cultured intestinal organoids [14]. We isolated intestinal crypts from bi-transgenic mice and assessed organoid morphology at different times following dox addition. I*n vitro* CRISPR induction for as little as 2 days led to the production of undifferentiated spheroids (Figure 2C, not shown) whose frequency increased with time. (Figure 2D). D7 dox-treated cultures were virtually 100% spheroid, and showed complete loss of full-length Apc protein with a corresponding increase in nonphosphorylated β-catenin, a downstream consequence of Apc loss (Figure 2E, Supplementary Figure 3B). Cultures derived from dox-treated c3GIC9-*Apc/Trp53* tandem mice showed near complete loss of p53 (Figure 2E and Supplementary Figure 3), further confirming the approach is effective for inactivation of multiple genes.

Interestingly, p53 expression in organoid cultures and intestine was mosaic, potentially reflecting in-frame deletions that do not cause loss of protein expression or cells that did not modify the *Trp53* locus (Figure 2A,E, Supplementary Figure 3). To comprehensively assess the frequency of indels produced following Cas9/Cas9n induction, we sequenced each target locus in gDNA from the intestine and thymus of dox-treated mice at an average depth of 55,000 reads/sample. Both tissues showed a high frequency (50-85%) of target gene modification following 10 days of dox (Figure 3A), although the size and types of indels varied significantly between each locus and tissue (Figure 3B, Supplementary Figure 4). Cas9n in combination with paired *Apc*-targeted sgRNAs showed a bias toward deletion events compared to the single *Apc*-targeted sgRNA (Supplementary Figure 4C), and a significant increase in deletion size (Figure 3B, Supplementary Figure 4A,D). Consistent with observations from ESCs, c3GIC9 tandem mice showed concordant mutation of both *Apc* and *Trp53* genes (Figure 3C, $R^2 = 0.972$).

Cas9 mutagenesis can produce both frameshift and in-frame indels that should, in principle, occur at a ratio of 2:1. Since in-frame deletions can produce functional proteins, the relative abundance of frameshift mutations in the tissue can indicate whether loss of gene function has a positive, negative or neutral impact on cell fitness. Consistent with this idea, Apc and Tp53 inactivation produce no selective advantage in ESCs, and both loci showed a predicted 2;1 ratio of frameshift to in frame deletions (Figure 1F). Conversely, Apc inactivation produces a substantial selective advantage in the intestine, and intestinal tissue from sgApc/Cas9 mice displayed a strong bias for Apc truncations (97% frameshift mutations) (Figure 3D). In these same animals, p53 inactivation produces little additional advantage in the time frame of analysis [15], and consequently the frequency of frameshift indels remained near the predicted 2/3 frequency (72%). Remarkably, while disruption of Apc conferred a strong selective advantage and disruption of p53 did not, both loci showed equivalent CRISPR-mediated modification (Figure 3A), implying that the system can be used to study 'fitness neutral' mutations.

As seen in ESCs and organoids, Cas9-induced mutagenesis *in vivo* was time dependent, as Cas9 expression for 4 days induced significantly less mutations and reduced overall disease burden in the intestine (Supplementary Figure 5). Thus, varying the duration of Cas9 expression by timing dox exposure provides a further level of control for altering gene function *in vivo*. Moreover, the ability to limit Cas9 expression may reduce toxicity and off-target effects associated with constitutive expression of sgRNA-Cas9 complexes, which can associate with thousands of genomic sequences [16].

In our system the spatial induction of mutagenesis is dictated by where the rtTA allele, and thus Cas9, is expressed. Hence, strategies that restrict rtTA to defined tissues provide a means to produce tissue specific gene disruption. To explore the potential for Cas9-induced genome editing in other tissues we used hydrodynamic transfection to express rtTA3 in a restricted and mosaic fashion in the liver of c3GIC9-Apc^{n} mice. Histological analyses showed expected cytoplasmic and nuclear accumulation of total and nonphosphorylated β-catenin specifically within GFP positive hepatocytes (Supplementary Figure 6). Thus, by controlling the expression of rtTA by either focused delivery (above) or using Cre-dependent systems[17], the CRISPR system can be adapted to producing tissue specific and conditional gene deletions *in vivo*. Taken together, our data show that dox-dependent Cas9 or Cas9n induction *in vivo* induces target gene alterations that can recapitulate the effects of traditional conditional knockout approaches.

Recent studies have described the application of CRISPR/Cas9-mediated genome editing *in vivo* using viral delivery or DNA transfection [18-21]. While enabling rapid CRISPR-based editing to produce gene modifications and chromosomal rearrangements, such methodologies are restricted to those tissues that can be efficiently accessed by exogenous constructs (i.e. liver, lung, brain). From a mouse-modelling standpoint, the iCRISPR platform is conceptually analogous to inducible Cre-based systems (i.e. CreER) though the effectiveness of each is difficult to directly compare. First, unlike the deletions created by LoxP-based alleles, CRISPR/Cas9 relies on imprecise DNA repair by NHEJ, and thus generates a heterogeneous population of genetic mutants. In theory, the frequency of 'null' alleles can be increased through the use of sgRNAs targeting the coding region of an

essential protein domain and/or using paired sgRNAs to increase deletion size (Figure 3B). Second, the efficiency of Cre-mediated deletion varies between genomic region and size of recombination event, whereas sgRNA sequence or variation in NHEJ efficiency may influence CRISPR/Cas9 mutagenesis. Importantly, we do not see the iCRISPR approach as replacing Cre/LoxP-based conditional knockouts, but rather providing a flexible and complementary alternative to study gene function *in vivo*, either when traditional methods are not applicable (e.g. for creating specific genetic truncations), or sufficiently rapid or scalable.

In *R26-rtTA* mice, TRE^{3G}-mediated Cas9 induction is strong in the intestine, skin, and thymus, and although the TRE^{3G} promoter shows some mosaicism in adult mice, given appropriate rtTA expression (e.g. by direct delivery or alternate transgenic strains) it can induce gene disruption in other tissues, such as the liver (Supplementary Figure 6). The incorporation of alternate TRE promoters or Cre-dependent TRE-LSL-Cas9 transgenes, analogous to those produced for tissue specific shRNA expression[17], should enable inducible mutagenesis in a wider range of tissues, thereby allowing tissue-restricted conditional gene disruption during development or in adults. Futhermore, the iCRISPR platform is adaptable CRISPR-mediated gene inhibition via transcriptional repression (CRISPRi) or activation (CRISPRa) using dCas9-KRAB and dCas9-VP64 variants, respectively [22,23]. These systems offer a powerful approach to simultaneously regulate the expression of multiple genes without mutational heterogeneity, however, they are yet to be fully evaluated *in vivo* and, unlike Cas9, do not induce the permanent genetic changes frequently associated with disease.

Finally, our work suggests that use of paired sgRNAs in combination with Cas9n can drive very robust loss-of-function phenotypes *in vivo* while reducing off-target mutagenesis, making it the system of choice for most applications. Although this approach requires the expression of 2 sgRNAs per target, the c3GIC9n targeting vector can accommodate at least six U6-sgRNA cassettes without significant loss of on-target efficiency (Supplementary Figure 7). Of course, increasing the number of genomic targets will also increase the complexity and heterogeneity of mutations, and thus, the analysis of strains that target many genes is likely to be complicated and best suited to cancer studies where such changes are positively selected. Regardless, inducible CRISPR/Cas9-mediated genome editing provides a simple strategy to develop conditional, genetic ‘deletion’ models in less than 6 months, providing a flexible, fast and low-cost platform to study gene function *in vivo*.

Online Methods

Animals

Production of mice and all treatments described were approved by the Institutional Animal Care and Use Committee (IACUC) at Memorial Sloan Kettering Cancer Center (NY), under protocol number 11-06-012. ES cell-derived mice were produced by blastocycst injection by the MSKCC transgenic core facility. Animals were maintained on a mixed C57B6/129 and progeny from breeding were genotyped for specific alleles (R26-rtTA and col1A1) using primers and protocols previously described [17,24]. Doxycycline was administered via food pellets (625mg/kg) (Harlan Teklad). Animal studies were not blinded. For detection of p53

protein, animals were sacrificed 4hrs following 6Gy whole body irradiation. For hydrodynamic plasmid delivery 12.5 μg of pCAGs-rtTA3 plasmid was mixed with sterile 0.9% sodium chloride solution. Mice were injected with a total amount of sodium chloride/ plasmid mix corresponding to 10 % of the body weight into the lateral tail vein within 5-7 seconds.

Cloning

hCas9 (from pX330) or hCas9n (pX335) was cloned into the *col1a1*-targeting vector downstream of the TRE3G-GFP-IRES. Sequences encoding guide RNAs were cloned into pX330 and pX335 for initial validation [1]. U6 promoter + guide RNA pairs were PCR amplified (sequences in Supplementary Table 3) and cloned (NsiI/SbfI) into an NsiI site upstream of the TRE3G promoter. The NsiI site reforms upstream of the U6-sgRNA cassette and can be used for sequential addition of sgRNAs. The *col1a1-TRE3G-GFP-IRES-Cas9* (c3GIC9) and c3GIC9n targeting vectors cannot be deposited at Addgene due to restrictions over distribution of plasmids containing the TRE3G promoter, but will be made available by request.

ES cell targeting

All ES cells were maintained on irradiated feeders in M15 media containing LIF as previously outlined [24]. Two days following transfections cells were treated with media containing 150ug/ml hygromycin and individual surviving clones were picked after 9-10 days of selection. Two days after clones were picked hygromycin was removed from the media and cells were cultures in standard M15 thereafter. To confirm single copy integration at the *col1a1* locus we first validated expected integration by multiplex *col1a1* PCR [24], and second, confirmed the presence of a single GFP cassette using the Taqman copy number assay, according to the manufacturers instructions (Invitrogen).

Immunohistochemistry and immunofluorescence

Tissue, fixed in freshly prepared 4% paraformaldehyde for 24 hours, was embedded in paraffin and sectioned by IDEXX RADIL (Columbia, MO). Sections were rehydrated and unmasked (antigen retrieval) by either: (i) Heat treatment for 10 mins in a pressure cooker in 10mM Tris / 1mM EDTA buffer (pH 9) containing 0.05% Tween 20 or (ii) Proteinase K treatment (200ug/ml) for 10 mins at 37C (Lysozyme staining). For immunohistochemistry, sections were treated with 3% H_2O_2 for 10 mins and blocked in TBS / 0.1% Triton X-100 containing 1% BSA. For immunofluorescence, sections were not treated with peroxidase. Primary antibodies, incubated at 4C overnight in blocking buffer, were: chicken anti-GFP (1:500, #ab13970), rabbit anti-ki67 (1:100, Sp6 clone, Abcam #ab16667), rabbit anti-KRT20 (1:250, Cell Signaling Technology, #13063), anti-Lysozyme (1:800, Dako, #EC3.2.1.17), rabbit anti-p53 (1:200, Leica Biosystems, #NCL-p53-CM5p) and rabbit anti-APC (1:150, Abcam #15270). For immunohistochemistry, sections were incubated with anti-rabbit ImmPRESS HRP-conjugated secondary antibodies (Vector Laboratories, #MP7401) and chromagen development performed using ImmPact DAB (Vector Laboratories, #SK4105). Stained slides were counterstained with Harris' hematoxylin. For immunofluorescent stains, secondary antibodies were applied in TBS for 1 hour at room

temp in the dark, washed twice with TBS, counterstained for 5 mins with DAPI and mounted in ProLong Gold (Life Technologies, #P36930). Secondary antibodies used were: anti-chicken 488 (1:500, DyLight IgG, #ab96947) and anti-rabbit 568 (1:500, Molecular Probes, #a11036). Images of fluorescent, ISH and IHC stained sections were acquired on a Zeiss Axioscope Imager Z.1 using a 10x (Zeiss NA 0.3) or 20x (Zeiss NA 0.17) objective and an ORCA/ER CCD camera (Hamamatsu Photonics, Hamamatsu, Japan). Raw .tif files were processed using Photoshop CS5 software (Adobe Systems Inc., San Jose, CA) to adjust levels and/or apply false coloring.

Isolation and culture of small intestinal organoids

Isolation—15 cm of the proximal small intestine was removed and flushed with cold PBS. After opening longitudinally it was washed in cold PBS until the supernatant was clear. The intestine was then cut into 5 mm pieces and placed into 10 ml cold 5mM EDTA-PBS and vigorously resuspended using a 10ml pipette. The supernatant was aspirated and replaced with 10ml EDTA and placed at 4°C on a benchtop roller for 10 minutes. This was then repeated for a second time for 30 minutes. The supernatant was aspirated and then 10ml of cold PBS was added to the intestine and resuspended with a 10ml pipette. After collecting this 10ml fraction of PBS containing crypts, this was repeated and each successive fraction was collected and examined underneath the microscope for the presence of intact intestinal crypts and lack of villi. The 10ml fraction was then mixed with 10ml DMEM Basal Media (Advanced DMEM F/12 containing Pen/Strep, Glutamine, B27 (Invitrogen 17504-044), 1mM N-Acetylcysteine (Sigma Aldrich A9165-SG)) containing 10 U/ml DNAse I (Roche, 04716728001) and filtered through a 100 micron filter into a BSA (1%) coated tube. It was then filtered through a 70 micron filter into a BSA (1%) coated tube and spun at 1200 RPM for 3 minutes. The supernatant was aspirated and the cell pellet mixed with 5ml Basal Media containing 5% FBS and centrifuged at 650 RPM for 5 minutes. The purified crypts were then resuspended in basal media and mixed 1:10 with Growth Factor Reduced Matrigel (BD, 354230). 40μl of the resuspension was plated in a 48 well plate and placed in a 37°C incubator to polymerize for 10 minutes. 250ul of small intestinal organoid growth media [Basal Media containing 50 ng/mL EGF (Invitrogen PMG8043), 100ng/ml Noggin (Peprotech 250-38), and 500 ng/mL R-spondin (R&D Systems, 3474-RS-050)] was then laid on top of the matrigel. Where appropriate, media was supplemented with 0.5ug/ml doxycycline (higher concentrations of dox are toxic to organoids).

Maintenance—Media was changed on organoids every two days and they were passaged 1:4 every 5-7 days. To passage, the growth media was removed and the Matrigel was resuspended in cold PBS and transferred to a 15ml falcon tube. The organoids were mechanically disassociated using a p1000 or a p200 pipette and pipetting 50-100 times. 7 ml of cold PBS was added to the tube and pipetted 20 times to fully wash the cells. The cells were then centrifuged at 1000 RPM for 5 minutes and the supernatant was aspirated. They were then resuspended in GFR matrigel and replated as above. For freezing, after spinning the cells were resuspended in Basal Media containing 10% FBS and 10% DMSO and stored in liquid nitrogen indefinitely.

Protein analysis

Small intestine organoids were grown in 300ul of Matrigel in 1 well each of a 6-well dish containing 3 mls of growth media for 4 days post-passage, then treated with 125ng/ml Adriamycin for 4 hrs to induce p53 expression. Organoids were then recovered from the Matrigel using several rinses with cold PBS. Organoid pellets were lysed with Lamelli buffer. Antibodies used for Western blot were: anti-APC (1:400, FE9 clone, Millipore #MABC202), anti-non-phosphorylated β-catenin (1:1000, #8814, Cell Signaling Technology), anti-p53 (1:500, #NCL-p53-505, Novocastra) and anti-actin-HRP (1:10,000, #ab49900, Abcam).

RNA isolation and QPCR

For small intestine samples. villi and crypts were harvested from the proximal duodenum (~1 inch) by scraping with a glass slide. Villi/crypt pellets were lysed with a wand homogenizer in 1mL of Trizol (Invitrogen, 15596-026) RNA was extracted according to the manufacturers instructions and contaminating DNA was removed by DNase treatment for 10 mins and column purification (Qiagen RNeasy). cDNA was prepared from 1 μg total RNA using Taqman reverse transcription kit (Applied Biosystems, #N808-0234) with random hexamers. Quantitative PCR detection was performed using SYBR green reagents (Applied Biosystems) using primers specific to Axin2, Lgr5, Myc (Supplementary Table 3).

Mutation detection by SURVEYOR assay

Cas9-induced mutations were detected using the SURVEYOR Mutation Detection Kit (Transgenomic/IDT). Briefly, an approximately 500bp region surrounding the expected mutation site was PCR-amplified using Herculase II (600675, Agilent Technologies). PCR products were column purified (Qiagen) and subjected to a series of melt-anneal temperature cycles with annealing temperatures gradually lowered in each successive cycle [25]. SURVEYOR nuclease was then added to selectively digest heteroduplex DNA. Digest products were visualized on a 2% agarose gel.

Sequence analysis

Sanger—c3GIC9-*Apc/Trp53* ESCs clones were treated with dox (1μg/ml) for 10 days, removed from dox for 2 days, then plated as single cells at low density and allowed to expand over 6 days. Individual ESC clones were picked directly into 15μl DNA lysis buffer (70mM Tris pH8.8, 160mM $(NH_4)_2SO_4$, 6.5mM $MgCl_2$, Proteinase K (400μg/ml)) and incubated at 55°C for 2hrs followed by 95°C for 20mins. Target regions were amplified from 1μl of crude gDNA using specific PCR primers (Supplementary Table 3) and sequenced by Dye terminator sequencing (Genewiz Inc., South Plainfield, NJ). In the case of non-homozygous indel events, overlapping sequences traces were deconvoluted using a 'CRISPR-Caller' algorithm (https://github.com/shackett/CRISPR-Caller/blob/master/CRISPR-Caller.R), modified to map to the mouse genome. Any traces that could not be deconvoluted to unambiguously identify two unique alleles (e.g. more than 2 peaks per position or unmappable regions) were excluded from further analysis.

MiSeq—Target regions were amplified from genomic DNA using specific PCR primers (Supplementary Table 3), amplicons were pooled in equimolar amounts and sequencing libraries were prepared using the Kapa Biosystems HTP library Preparation kit (cat# kk8234), strictly following the manufacturers instructions. Barcoded libraries were pooled into a 150bp/150bp paired end MiSeq run, using the TruSeq SBS Kit v3 (Illumina). To look for insertion/deletion events, the sequence data (FASTQ files) were mapped to the mouse (MM10) genome using BWA version 0.7.10 (bwa mem -M). The output SAM files were then directly processed to filter for one of the reads in the pair and also filtered for mapq ≥ 50. In this read set we directly scanned the cigar string for either 1) reads that were predicted length (150bp) or 2) reads that contained one, and only one insertion (I) or deletion (D) event. 150bp reads that were counted as WT and for reads containing an indel, we extracted the length of the event and stored a histogram of indel lengths. The final output was a count of the total number of reads that passed filtering broken down in those with and without indels. Due to relatively high error rate inherent to the sequencing throughout the length of the reads, single base substitutions were ignored and scored as WT. This may have resulted in slight overestimation of the frequency of WT reads.

Off-target predictions

We identified 20mer sequences in the mouse genome that showed complete or partial identity to the primary Apc and Trp53-targeted sgRNAs according to the following criteria: up to 1 mismatch in the 12bp seed region immediately adjacent to the 3' NGG PAM sequence, and up to 5 mismatches in the 8bp region at the 5' end of the sgRNA. To do this we used the SHRiMP mapper (gmapper-ls) searching for all gapless alignments with 30% alignment score against the full mouse genome. This list was then post-processed to filter matches for the above mismatch criteria. For each predicted region we designed PCR primers surrounding the site and assessed indel formation by Surveyor assay.

Supplementary Material

Refer to Web version on PubMed Central for supplementary material.

Acknowledgements

We thank Janelle Simon for technical assistance with animal colonies, and other members of the Lowe laboratory for advice and discussions. We thank the MSKCC transgenic core facility for production of transgenic animals by blastocyst injection and the MSKCC Genomics core facility for library preparation and Illumina sequencing. This work was supported by a program project grant from the National Cancer Institute (NCI). LED was supported by a K22 Career Development Award from the NCI/NIH under award number 1K22CA181280-01. KPO was supported by a Medical Scientist Training Program grant from the National Institute of General Medical Sciences of the National Institutes of Health under award number T32GM07739 to the Weill Cornell / Rockefeller / Sloan-Kettering Tri-Institutional MD-PhD Program. GL was supported by an American Cancer Society postdoctoral fellowship PF-13-037-01 and NIH F32 grant 1F32CA177072-01. SWL is an investigator of the Howard Hughes Medical Institute and the Geoffrey Beene Chair for Cancer Biology.

References

1. Cong L, et al. Multiplex genome engineering using CRISPR/Cas systems. Science. 2013; 339:819–823. [PubMed: 23287718]
2. Mali P, et al. RNA-guided human genome engineering via Cas9. Science. 2013; 339:823–826. [PubMed: 23287722]

3. Ran FA, et al. Double nicking by RNA-guided CRISPR Cas9 for enhanced genome editing specificity. Cell. 2013; 154:1380–1389. [PubMed: 23992846]
4. Li D, et al. Heritable gene targeting in the mouse and rat using a CRISPR-Cas system. Nat Biotechnol. 2013; 31:681–683. [PubMed: 23929336]
5. Wang H, et al. One-step generation of mice carrying mutations in multiple genes by CRISPR/Cas-mediated genome engineering. Cell. 2013; 153:910–918. [PubMed: 23643243]
6. Yang H, et al. One-step generation of mice carrying reporter and conditional alleles by CRISPR/Cas-mediated genome engineering. Cell. 2013; 154:1370–1379. [PubMed: 23992847]
7. Hochedlinger K, Yamada Y, Beard C, Jaenisch R. Ectopic expression of Oct-4 blocks progenitor-cell differentiation and causes dysplasia in epithelial tissues. Cell. 2005; 121:465–477. [PubMed: 15882627]
8. Premsrirut PK, et al. A rapid and scalable system for studying gene function in mice using conditional RNA interference. Cell. 2011; 145:145–158. [PubMed: 21458673]
9. Moser AR, et al. Homozygosity for the Min allele of Apc results in disruption of mouse development prior to gastrulation. Dev Dyn. 1995; 203:422–433. [PubMed: 7496034]
10. Su LK, et al. Multiple intestinal neoplasia caused by a mutation in the murine homolog of the APC gene. Science. 1992; 256:668–670. [PubMed: 1350108]
11. Gonzalez F, et al. An iCRISPR platform for rapid, multiplexable, and inducible genome editing in human pluripotent stem cells. Cell Stem Cell. 2014; 15:215–226. [PubMed: 24931489]
12. Fu Y, et al. High-frequency off-target mutagenesis induced by CRISPR-Cas nucleases in human cells. Nat Biotechnol. 2013; 31:822–826. [PubMed: 23792628]
13. Sansom OJ, et al. Loss of Apc in vivo immediately perturbs Wnt signaling, differentiation, and migration. Genes Dev. 2004; 18:1385–1390. [PubMed: 15198980]
14. Sato T, et al. Long-term expansion of epithelial organoids from human colon, adenoma, adenocarcinoma, and Barrett's epithelium. Gastroenterology. 2011; 141:1762–1772. [PubMed: 21889923]
15. Reed KR, et al. A limited role for p53 in modulating the immediate phenotype of Apc loss in the intestine. BMC cancer. 2008; 8:162. [PubMed: 18533991]
16. Wu X, et al. Genome-wide binding of the CRISPR endonuclease Cas9 in mammalian cells. Nat Biotechnol. 2014; 32:670–676. [PubMed: 24752079]
17. Dow LE, et al. Conditional reverse tet-transactivator mouse strains for the efficient induction of TRE-regulated transgenes in mice. PLoS ONE. 2014; 9:e95236. [PubMed: 24743474]
18. Maddalo D, et al. In vivo engineering of oncogenic chromosomal rearrangements with the CRISPR/Cas9 system. Nature. 2014; 516:423–7. [PubMed: 25337876]
19. Platt RJ, et al. CRISPR-Cas9 Knockin Mice for Genome Editing and Cancer Modeling. Cell. 2014; 159:440–455. [PubMed: 25263330]
20. Sanchez-Rivera FJ, et al. Rapid modelling of cooperating genetic events in cancer through somatic genome editing. Nature. 2014; 516:428–31. [PubMed: 25337879]
21. Xue W, et al. CRISPR-mediated direct mutation of cancer genes in the mouse liver. Nature. 2014; 514:380–384. [PubMed: 25119044]
22. Gilbert LA, et al. CRISPR-mediated modular RNA-guided regulation of transcription in eukaryotes. Cell. 2013; 154:442–451. [PubMed: 23849981]
23. Qi LS, et al. Repurposing CRISPR as an RNA-guided platform for sequence-specific control of gene expression. Cell. 2013; 152:1173–1183. [PubMed: 23452860]
24. Dow LE, et al. A pipeline for the generation of shRNA transgenic mice. Nature Protocols. 2012; 7:374–93. [PubMed: 22301776]
25. Sanjana NE, et al. A transcription activator-like effector toolbox for genome engineering. Nat Protoc. 2012; 7:171–192. [PubMed: 22222791]

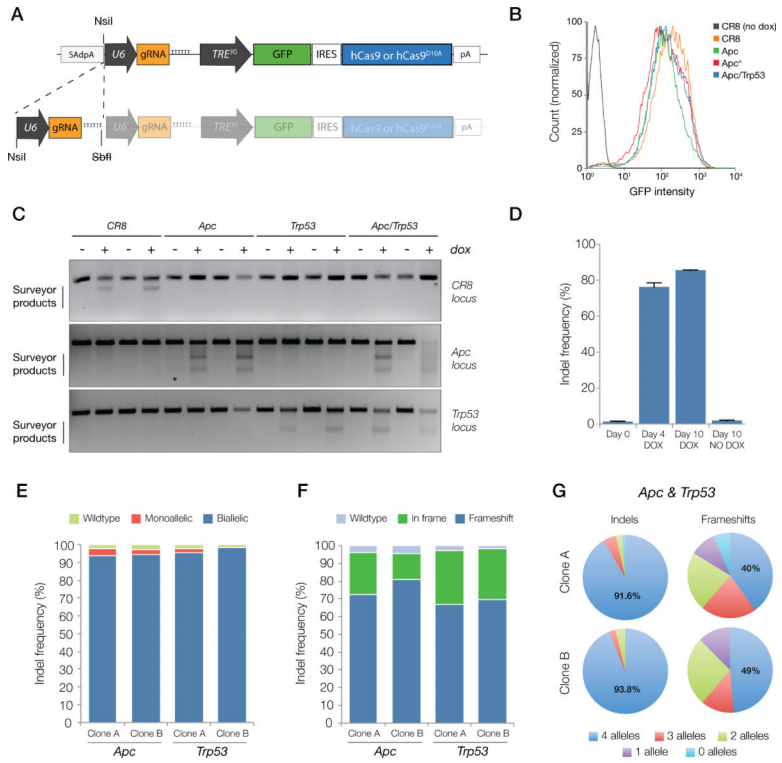

Figure 1.

Inducible genome editing in mESCs. **A**. Schematic representation of the c3GIC9 *col1a1*-targeting vector. U6-sgRNA cassettes are cloned (NsiI/SbfI) into a unique NsiI site, recreating the NsiI site upstream of the U6 promoter, allowing addition of further U6-sgRNA modules. **B**. GFP induction in ES cell clones 72 hrs following 1μg/ml dox treatment. **C.** Surveyor assay of the *CR8*, *Apc* and *Trp53* loci following 2 days of dox treatment of individual targeted ES cell clones (2 clones shown per genotype). Asterisk indicates detectable mutation events in the absence of dox observed in some clones. **D**. Indel frequency at the Apc locus in transgenic c3GIC9-*Apc/Trp53* ESCs culture with or without 1μg/ml dox as indicated (Error bars are SEM, n = 2). **E**. Frequency of wild-type, mono-allelic or bi-allelic indels at the *Apc* and *Trp53* loci in c3GCI9-*Apc/Trp53* ESCs treated with dox for 10 days, then expanded as individual clones in the absence of dox (clone A, n = 83; Clone B, n = 71). **F**. Frequency of frameshift (blue) and in-frame mutations (green) at the *Apc* and *Trp53* loci in ESC clones described in **E**. **G**. Pie charts representing the frequency of indels (left) and frameshift mutations (right) at both *Apc* and *Trp53*, showing 91-94% of clones carry bi-allelic indels at both loci and 40-49% carry frameshift mutations in all 4 alleles.

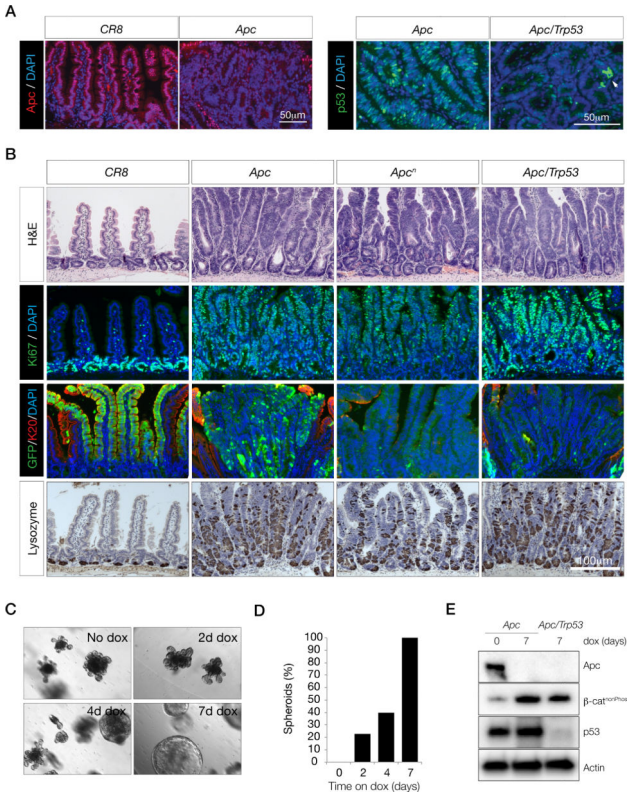

Figure 2.

Inducible genome editing in adult mice. **A.** Immunofluorescent stains of intestinal sections from 10-day dox-treated R26-rtTA / c3GIC9-*CR8*, *Apc*, and *Apc/Trp53* mice, as indicated. Sections, stained for Apc (red), and p53 (green) show loss of each target protein following dox treatment. White arrow indicates rare clusters of 'p53 high' cells in dox-treated c3GCI9-*Apc/Trp53* animals. Scale bars are 50μm. **B**. Immunohistochemical and immunofluorescent images of intestinal sections from 10-day dox-treated R26-rtTA / c3GIC9-*CR8*, *Apc*, *Apc/Trp53* and c3GIC9n-*Apc* (*Apc*^{n}) mice. Sections were stained for markers of proliferation (Ki67-green), differentiation (K20 – red) and Paneth cells (Lysozyme – brown). Induction of Apc-targeted sgRNAs results in hyperplastic overgrowth, blocked differentiation and ectopic production of Paneth cells. Scale bars are 100μm **C**. Brightfield images of organoid cultures from R26-rtTA / c3GIC9-*Apc* transgenic mice treated with dox (0.5μg/ml) for 0, 2 4, or 7 days then expanded in culture for 10 days. **D**. Quantitation of spheroid formation in cultures in **C**. Bars represent the percentage of spheres (vs. normal organoids) 10 days following the withdrawal of dox. **E**. Western blot of whole cell lysates from c3GIC9-*Apc* and c3GIC9-*Apc/Trp53* organoid cultures treated with dox as indicated shows loss of full-length Apc, an increase in non-phosphorylated β-catenin, reflecting elevated signaling following loss of Apc protein, and deletion of p53 protein only in c3GIC9-*Apc/Trp53* cells. An uncropped, full-length image of the Apc blot is presented in Supplementary Figure 3, showing expression of the truncated protein following CRISPR-mediated editing.

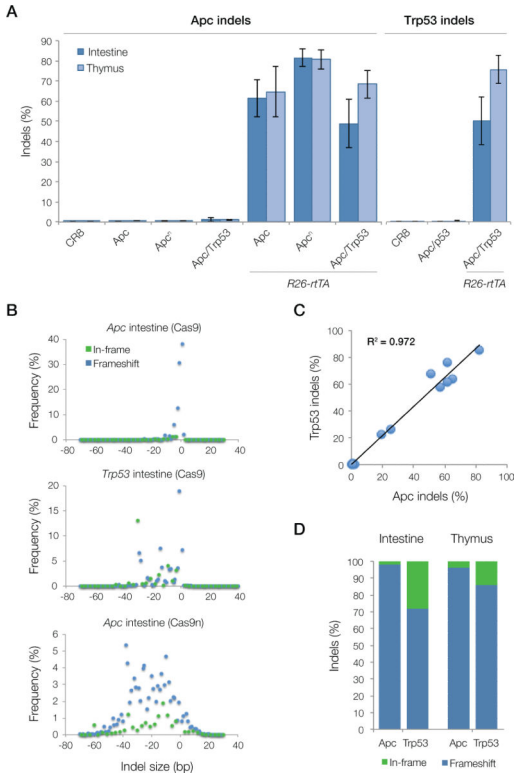

Figure 3.

Frequency and type of gene modifications following Cas9/Cas9n induction in mice. **A.** Frequency of indels in the intestine (dark blue) and thymus (light blue) in control (*CR8*), dox-naïve (no R26-rtTA) and D10 dox-treated mice at the *Apc* and *Trp53* loci, as indicated (Error bars are SEM, n ≥ 3). **B**. Scatter plots displaying frequency and size of indels at the *Apc* and *Trp53* loci in dox-treated intestine, as indicated. Blue points indicate frameshift mutations while green points indicate in-frame indels (n=4). **C**. Scatter plot showing a correlation of the frequency of *Apc* and *Trp53* indels in c3GIC9-*Apc/Trp53* tandem mice. Data from both intestine and thymus is shown together. **D**. Frequency of frameshift (blue) and in-frame indels (green) in the intestine and thymus of dox-treated mice, as indicated (n=4 for each locus and each tissue)